General Disclaimer

One or more of the Following Statements may affect this Document

- This document has been reproduced from the best copy furnished by the organizational source. It is being released in the interest of making available as much information as possible.

- This document may contain data, which exceeds the sheet parameters. It was furnished in this condition by the organizational source and is the best copy available.

- This document may contain tone-on-tone or color graphs, charts and/or pictures, which have been reproduced in black and white.

- This document is paginated as submitted by the original source.

- Portions of this document are not fully legible due to the historical nature of some of the material. However, it is the best reproduction available from the original submission.

NATIONAL AERONAUTICS AND SPACE ADMINISTRATION

Technical Memorandum 33-487

Volume I

Use of Centaur Spacecraft Flight Data in the Synthesis of Forcing Functions at Centaur Main Engine Cutoff During Boost of Mariner Mars 1969, OAO-II, and ATS Spacecraft: Analysis and Evaluation

M. R. Trubert

J. R. Chisholm

W. H. Gayman

JET PROPULSION LABORATORY

CALIFORNIA INSTITUTE OF TECHNOLOGY

PASADENA, CALIFORNIA

June 21, 1971

NATIONAL AERONAUTICS AND SPACE ADMINISTRATION

Technical Memorandum 33-437

Volume I

Use of Centaur Spacecraft Flight Data in the Synthesis of Forcing Functions at Centau. Main Engine Cutoff During Boost of Mariner Mars 1969, OAO-II, and ATS Spacecraft: Analysis and Evaluation

M. R. Trubert

J. R. Chisholm

W. H. Gayman

JET PROPULSION LABORATORY

CALIFORNIA INSTITUTE OF TECHNOLOGY

PASADENA, CALIFORNIA

June 21, 1971

ACKNOWLEDGEMENT

The numerical analyses leading to the synthesis of Centaur engine forcing functions were funded by NASA Langley Research Center and were under the cognizance of Dr. John P. Raney and Mr. Larry D. Pinson. The work described in this document was performed by the Engineering Mechanics Division of the Jet Propulsion Laboratory.

CONTENTS

CONTENTS (Cont'd)

Figures (Cont'd)

Tables

Tables (Cont'd)

ABSTRACT

Acceleration flight data of Mariner Mars '69, OAO-II and ATS spacecraft in the boost phase were used to determine the disturbing forcing function of the Centaur engines at Main Engine Cutoff event. An inverse solution using the concept of Fourier transform and transfer function is presented. Mathematical dynamic models of the spacecraft and the Centaur launch vehicle were derived and Fourier transforms and time histories of the disturbing forcing function were determined. Analysis to determine the response and reaction forces and moments of another spacecraft using the same Centaur vehicle has been derived.

I. INTRODUCTION

Through a cooperative effort among NASA Lewis Research Center, NASA Goddard Space Flight Center and the Jet Propulsion Laboratory, similar sets of acceleration measurements were obtained through continuous telemetry during the launch and exit phases of six spacecraft having Atlas/Centaur launch vehicles. These spacecraft were two Mariner Mars '69 (Mariners VI and VII), two OAO-II and two ATS. Only one OAO-II is reported in this memorandum.

Ref. 1 describes the instrumentation and the data processing leading to the obtaining of phase-coherent acceleration-time histories, i.e., three translational and three rotational components measured in a plane at the field joint in the spacecraft adapter structure. This description relates specifically to analysis of Mariner data, but the method of processing applies generally to the other spacecraft.

This memorandum deals with the use of the observed acceleration responses at Centaur Main Engine Cutoff (MECO) in deriving the engine forcing functions that produced the responses. The steps in this process entailed the following:

1. Computation of the Fourier transform $\{A(\omega)\}$ of each acceleration transient.
2. Computation of the three-dimensional normal modes of each composite space vehicle for the configuration at MECO.
3. Computation of the structural transfer function matrix $[H(\omega)]$ relating the Fourier transform $\{A(\omega)\}$ of the acceleration response at the plane of the flight accelerometers to the Fourier transform $\{F(\omega)\}$ of the force vector at the main engine gimbal-block station.
4. Use of the inverse transfer function $[H(\omega)]^{-1}$ to obtain the Fourier

transform of the force vector, $\{F(\omega)\}$.

5. Use of the inverse Fourier transform to convert the forcing functions from the frequency domain to the time domain.

This memorandum also derives the equations for obtaining the acceleration components and the reaction forces and moments at the base of any spacecraft in a Centaur/spacecraft combination at MECO, from the derived forcing functions, $\{f(t)\}$. Again, the solution is indicated in the frequency domain, with conversion to the time domain when appropriate.

Ref. 2 applies the methods and analyses of this memorandum to the predictions of base accelerations and reactions of Mariner Mars '71 and Viking spacecraft at MECO.

II. MATHEMATICAL ANALYSIS

A. Determination of the Forcing Function

The measurement of six accelerations $u_1(t)$, $u_2(t)$,..., $u_6(t)$ at six locations of the base of the spacecraft furnishes enough inputs to determine six components of a forcing function $f_1(t)$, $f_2(t)$,...,$f_6(t)$ applied at a given location A_1 of the launch vehicle (Fig. 1).

The six accelerations $u_1(t)$, $u_2(t)$,..., $u_6(t)$ were three axial and three tangential accelerations and were measured at the field joint for Mariner Mars '69, OAO-II and ATS spacecraft. For a more meaningful display of the data the six accelerations $u_1(t)$, $u_2(t)$,..., $u_6(t)$ were reduced to three translations $a_1(t)$, $a_2(t)$, $a_3(t)$ and three rotations $a_4(t)$, $a_5(t)$, $a_6(t)$ at the center A_2 of the field joint on the z axis (Fig. 2). Assuming a perfectly rigid field joint, we have

$$\{a^1(t)\} = [T]\{u(t)\} \qquad (1)$$

where [T] is a 6 x 6 matrix obtained from the geometry of the accelerometer placement. Details of the derivation and solution of Eq. (1) are presented in Ref. 1.

A frequency domain solution of the problem has been used representing a generalization of the method of Ref. 3. The dynamic characteristics of the total structure made of the combined Centaur/spacecraft (Fig. 1) are represented by N free-free normal modes. The equations of motion for the system in terms of the free-free modes are

$$[M_{rr}]\{\ddot{r}\} = [\phi_{1r}]^T\{f\} \qquad (2)$$

for the rigid body modes and

$$\lceil M_{ee} \rfloor\{\ddot{q}\} + \lceil C_{ee} \rfloor\{\dot{q}\} + \lceil K_{ee} \rfloor\{q\} = [\phi_{1e}]^T\{f\} \qquad (3)$$

for the elastic modes. The acceleration response $\{a^1\}$ is given by

$$\{a^1\} = [\phi_{2r} | \phi_{2e}]\begin{Bmatrix}\ddot{r}\\ \ddot{q}\end{Bmatrix} \qquad (4)$$

In Eqs. (2) through (4)

$[M_{rr}]$ is the rigid body mass matrix (6 x 6) (mass, static unbalance and inertia) with respect A_1

$\lceil M_{ee} \rfloor$ is the generalized mass matrix (diagonal N x N)

$\lceil C_{ee} \rfloor$ is the generalized damping matrix (diagonal N x N)

$\lceil K_{ee} \rfloor$ is the generalized stiffness matrix (diagonal N x N)

$\{r\}$ is the column of the displacement of the rigid body modes (6 x 1)

$\{q\}$ is the column of elastic generalized displacements (N x 1)

$[\phi_{1r}]$ is the rigid body mode shape at point A_1 (6 x 6)

$[\phi_{1e}]$ is the elastic mode shape at point A_1 (6 x N)

$[\phi_{2r}]$ is the rigid body mode shape at point A_2 (6 x 6)

$[\phi_{2e}]$ is the elastic mode shape at point A_2 (6 x N)

$\{f\}$ is the column of forces and moments at point A_1

$\{a^1\}$ is the column of the accelerations at point A_2

Then we take the Fourier transform of both sides of Eqs. (2) through (4). By convention capital letters for the columns will mean Fourier transform i.e., for example,

$$\{A^1(\omega)\} = \int_{-\infty}^{+\infty} \{a^1(t)\} e^{-i\omega t} dt \tag{5}$$

where $i = \sqrt{-1}$. Similar expressions hold for $\{r\}$, $\{q\}$ and $\{f\}$.

Eqs. (2) through (4) become the following algebraic equations:

$$-\omega^2 [M_{rr}]\{R\} = [\phi_{1r}]^T \{F\} \tag{6}$$

$$[-\omega^2 M_{ee} + i\omega C_{ee} + K_{ee}]\{Q\} = [\phi_{1e}]^T \{F\} \tag{7}$$

$$\{A^1\} = -\omega^2 [\phi_{2r} | \phi_{2e}] \left\{\frac{R}{Q}\right\} \tag{8}$$

Next we solve the algebraic Eqs. (6) and (7) for $\{R\}$ and $\{Q\}$ and substitute into Eq. (8) to obtain the following input-output relationship (Fig. 3)

$$\{A^1(\omega)\} = [H^1(\omega)]\{F(\omega)\} \tag{9}$$

where $[H^1(\omega)]$ is the transfer function matrix

$$[H^1(\omega)] = [\phi_{2r} M_{rr}^{-1} \phi_{1r} + \phi_{2e} Z^{-1} \phi_{1e}] \tag{10}$$

in which [Z] is a frequency dependent diagonal complex matrix (N x N)

$$\lceil Z \rfloor = \lceil Z_n(\omega) \rfloor \tag{11}$$

Each term Z_n of Eq. (11) is

$$Z_n = \mu_n \left(1 - \frac{\omega^2}{\omega_n^2} - 2i\xi_n \frac{\omega}{\omega_n}\right) \tag{12}$$

where μ_n, ω_n, ξ_n are the generalized mass, the natural frequency and the modal damping of each free-free mode, respectively.

The forcing function $\{F(\omega)\}$ is obtained by inverting the 6 x 6 transfer function matrix $[H_1(\omega)]$, i.e.,

$$\{F(\omega)\} = [H^1(\omega)]^{-1}\{A^1(\omega)\} \tag{13}$$

The time history of the forcing function $\{f(t)\}$ is obtained by inverse Fourier transform

$$\{f(t)\} = \frac{1}{2\pi}\int_{-\infty}^{+\infty} \{F(\omega)\}e^{i\omega t}d\omega \tag{14}$$

B. Response of Another Spacecraft

We now assume that the flight spacecraft (Mariner'69, OAO and/or ATS) are removed from the Centaur vehicle and replaced by another spacecraft. Eqs. (2) through (12) still hold except that the modes are those corresponding to the new Centaur/spacecraft configuration. The acceleration response at the base of the spacecraft (Fig. 4) is given by

$$\{A^2(\omega)\} = [H^2(\omega)]\{F(\omega)\} \tag{15}$$

where $[H^2(\omega)]$ is the transfer function matrix given by Eq. (10) in which the modes correspond to the Centaur/new spacecraft combination.*

---

*In Eq. (15) as in the following equations 2 is a superscript not a power of two; the only exception is for ω in the later equations.

C. Determination of Reaction Forces and Moments at the Base of the Spacecraft

Once the base acceleration of a spacecraft $\{a^2(t)\}$ in the boost configuration on the launch vehicle is known, the reaction forces and moments $\{g(t)\}$ at a point A_3 of the base of the spacecraft can be determined. The first M cantilevered normal modes are used to represent the structural characteristics of the spacecraft. The equations of motion are (Refs. 4,5

$$\left[\begin{array}{c|c} M_{RR} & M_{RE} \\ \hline M_{ER} & M_{EE} \end{array}\right]\left\{\begin{array}{c} \ddot{x}^2 \\ \hline \ddot{p} \end{array}\right\} + \left[\begin{array}{c|c} 0 & 0 \\ \hline 0 & C_{EE} \end{array}\right]\left\{\begin{array}{c} \dot{x}^2 \\ \hline \dot{p} \end{array}\right\} + \left[\begin{array}{c|c} 0 & 0 \\ \hline 0 & K_{EE} \end{array}\right]\left\{\begin{array}{c} x^2 \\ \hline p \end{array}\right\} = \left\{\begin{array}{c} g \\ \hline 0 \end{array}\right\} \qquad (16)$$

where:

$[M_{RR}]$ is the rigid body matrix (6 x 6) of the spacecraft with respect to the base at point A_3

$[M_{RE}]$ is the rigid elastic matrix (6 x M) with respect to point A

$[M_{ER}]$ $= [M_{RE}]^T$

$\lceil M_{EE} \rfloor$ is the generalized mass matrix (M x M)

$\lceil C_{EE} \rfloor$ is the generalized damping matrix (M x M)

$\lceil K_{EE} \rfloor$ is the generalized stiffness matrix (M x M)

$\{p\}$ is the column of the generalized displacement with respect the base

$\{x^2\}$ is the column of the base motion at point A_3

$\{g\}$ is the column of the reaction forces and moments

Expanding Eq. (16) we obtain

$$[M_{RR}]\{\ddot{x}^2\} + [M_{RE}]\{\ddot{p}\} = \{g\} \qquad (17)$$

$$[M_{ER}]\{\ddot{x}^2\} + \lceil M_{EE} \rfloor\{\ddot{p}\} + \lceil C_{EE} \rfloor\{\dot{p}\} + \lceil K_{EE} \rfloor\{p\} = 0 \qquad (18)$$

The differential Eqs. (17) and (18) are then transformed into algebraic equations by Fourier transform

$$-\omega^2 [M_{RR}]\{X^2\} - \omega^2 [M_{RE}]\{P\} = \{G\} \tag{19}$$

$$-\omega^2 [M_{ER}]\{X^2\} + [-\omega^2 M_{EE} + i\omega C_{EE} + K_{EE}]\{P\} = 0 \tag{20}$$

The Fourier transform of the acceleration $\{A^2(\omega)\}$ is related to the displacement $\{X^2(\omega)\}$ by

$$\{A^2(\omega)\} = -\omega^2\{X^2(\omega)\} \tag{21}$$

Solving Eq. (20) for $\{P\}$ and substituting into Eq. (19) we obtain

$$[M_{RR} - M_{RE}Y^{-1}M_{ER}]\{A^2(\omega)\} = \{G(\omega)\} \tag{22}$$

where [Y] is a frequency-dependent diagonal complex matrix (M x M) identical in form to Eqs. (11) and (12) except that the parameters are relative to the cantilevered modes

$$\lceil Y \rfloor = \lceil Y_m(\omega) \rfloor \tag{23}$$

$$Y_m(\omega) = \nu_m\left(1 - \frac{\omega_m^2}{\omega^2} - 2i\xi_m\frac{\omega_m}{\omega}\right) \qquad m = 1,2,\ldots,M \tag{24}$$

Call $[H^3(\omega)]$ the transfer function matrix premultiplying $\{A^2(\omega)\}$ in Eq. (22); we have

$$[H^3(\omega)] = [M_{RR} - M_{RE}Y^{-1}M_{ER}] \tag{25}$$

$$\{G(\omega)\} = [H^3(\omega)]\{A^3(\omega)\} \tag{26}$$

The expression of Eq. (25) is similar to Eq. (10) and the same computer program can be used to calculate Eq. (25) provided one makes the following identities

$$[\phi_{2r}] \equiv [M_{RR}] \tag{27}$$

$$[M_{rr}] \equiv [\phi_{1r}] \equiv [1] \tag{28}$$

$$[\phi_{2e}] \equiv [-M_{RE}] \tag{29}$$

$$[\phi_{1e}] \equiv [M_{ER}] \tag{30}$$

$$[Z] \equiv [Y] \tag{31}$$

The time histories of the reaction forces and moments are again obtained by inverse Fourier transform using Eq. (14) replacing $\{F(\omega)\}$ by $\{G(\omega)\}$.

The numerical application of the analysis of the last two sections, B and C, will not be done in this memorandum but will be presented in a companion memorandum (Ref. 2).

D. Requirements and Assumptions

The above derivation to be successfully utilized in practice requires three conditions that are difficult to meet:

a) the location of the disturbance (here the Centaur main engine gimbal plane) is well known.

b) the mathematical model represented by Eqs. (2) through (4) is sufficiently descriptive for the structure, especially in the region where the data are measured and where the disturbing forcing function is assumed to be applied.

c) the measured data are reliable, i.e., free of amplitude and phase distortion, telemetry noise and drift.

It should be noted that only one equivalent load (force and moment) which reproduces the measured data through the assumed model is obtained. Separating the equivalent load into the actual thrusts at the two engines would require a detail modeling of the engines which was not available here. It was assumed in the present study that this equivalent load when applied to another spacecraft using the same vehicle, would give a good estimate of the response at the base of the spacecraft.

III. MATHEMATICAL MODELS

A. Centaur Launch Vehicle Model

The basic Centaur model was obtained from Ref. 6 which describes models of the Atlas/Centaur SLV-3C launch vehicle. The original GDC model is shown on Fig. 5. This model was modified to incorporate an improved model of the engines in a manner similar to that of Ref. 7. The resulting JPL model is given in Figs. 5 through 7. Tables 1 through 6 give weight and stiffness properties for the Centaur model which was used with the Mariner '69, OAO-II and ATS spacecraft.

B. Mariner-Mars '69 Spacecraft Model

The model used for the Mariner spacecraft was represented by normal modes of the spacecraft (including the Centaur adapter) cantilevered at the base of the Centaur adapter. The mass matrix $[M_{RR}]$, the elastic-rigid coupling matrix $[M_{ER}]$ and natural frequencies $[\omega_n]$ were obtained from previous analysis performed at JPL. Those matrices are shown in Tables 7 and 8.

C. OAO-II Spacecraft Model

A simple structural model for the OAO-II spacecraft, furnished by Goddard Space Flight Center through Grumman Aircraft Engineering Company, was used for the modal analysis. The model consisted of nine mass points connected by eight spring elements (Fig. 8). The data for the lumped parameter model, revised as of July 30, 1968, consisted of nine translational and rotational inertia values (Table 9), and eight axial, torsional bending and shear compliances (Table 10). The model also contained the associated Grumman Aircraft Engineering Company (GAEC) vehicle station numbers.

D. ATS Spacecraft Model

The ATS model was furnished by TRW and consisted of twenty-three lumped masses connected by springs as represented in Fig. 9. The stiffnesses, inertia properties and coordinate data of this model are given in Tables 11 and 12.

IV. COMPUTER ANALYSIS AND RESULTS

A. Computer Programs

The JPL SAMIS computer program (Ref. 8) was used to compute the normal modes needed for the numerical computation of the transfer function matrix $[H^1(\omega)]$. The JPL RECEP computer program (Ref. 9) was used for the numerical computation of Eqs.(5), (10), (13) and (14). Considerations on the use of the fast Fourier transform algorithm used in this program are given in Ref. 4, Appendix B. The reduced flight data $\{a^1(t)\}$ were digitized from the analog signals and stored on magnetic tape. This tape was used as an input to the RECEP program.

B. Mariner-Mars '69/Centaur Composite Vehicle

The normal modes and attachment modes of the Centaur vehicle were obtained considering the vehicle cantilevered at the gimbal axis (gridpoint 67, Fig. 5) and generalized mass and stiffness matrices were generated. Attachment modes as described in Ref. 10 were generated at the separation plane between Centaur and spacecraft so that the Mariner spacecraft could be attached to the Centaur to form a composite model. The $[M_{RR}]$, $[M_{ER}]$ and $\lceil \omega_n \rfloor$ terms of the Mariner model were combined with the generalized mass and stiffness matrices of the vehicle to form the composite vehicle-spacecraft model. The free-free normal modes $[\phi_{1e}]$, $[\phi_{2e}]$, $\lceil \omega_n \rfloor$ of the composite model were obtained in order to compute Eqs. (10) through (12).

The normalization of the modes was such that the generalized mass μ_n was unity.

The rigid body mass properties $[M_{rr}]$ needed for Eq. (10) were also obtained from this composite model. The rigid body modes $[\phi_{1r}]$ and $[\phi_{2r}]$ were obtained by applying unit translations (1 inch) and unit rotations (1 radian) at point A_1 for three directions (Fig. 1). Tables 13 and 14 show $[\phi_{1r}]$, $[\phi_{2r}]$, $\lceil \omega_n \rfloor$, $[\phi_{1e}]$ and $[\phi_{2e}]$ matrices. Table 15 shows the $[M_{rr}]$ matrix. A modal damping of $\xi_n = .03$ was chosen for all modes.

Eq. (10) was then solved using the RECEP program to obtain the transfer function $[H^1(\omega)]$ between the separation plane (gridpoint 12, Fig. 5) and the gimbal axis (gridpoint 67, Fig. 5). The six components of the measured separation plane acceleration data relative to the two Mariner '69 flights (AC-20 Mariner VI and AC-19 Mariner VII) were digitized and the Fourier transforms computed by Eq. (5). Figs. A-1 through A-12 of Vol. II show the time histories and the corresponding Fourier transforms of these flight data.

The six components of the forcing function $\{f(t)\}$ at the gimbal axis were then computed by Eqs. (13) and (14) using the above flight acceleration data. The time histories and the Fourier transforms of the forcing function are given in Figs. A-13 through A-24.

C. OAO-II/Centaur Composite Vehicle

Within the overall launch vehicle system the OAO-II spacecraft is represented by gridpoints 1 through 9 of Fig. 8. The Centaur model of Fig. 5 was modified for the OAO by the addition of five mass points connected by four spring elements to represent the conical and transition adapters between the Centaur and the OAO spacecraft. These five mass points are indicated in Fig. 8.

The composite vehicle consisted of two substructure models:

(a) The combination of the OAO-II spacecraft and the OAO/Centaur conical adapter cantilevered at gridpoint 20 in Fig. 8.

(b) The Centaur model cantilevered at the gimbal axis, gridpoint 67 in Fig. 8.

The cantilevered normal modes of each part of the composite vehicle were obtained using the SAMIS program (Ref. 8). The two submodels were then combined using the substructural approach of Ref. 10 to obtain the free-free overall vehicle modes. The modal data are shown in Tables 16, 17 and 18. The forcing function $\{f(t)\}$ was obtained using the RECEP program in a manner identical to the Mariner/Centaur composite vehicle.

Frequency domain computations similar to section B were performed using the above modal data and a modal damping $\xi_n = .03$ for all modes. The time histories and the corresponding Fourier transforms of the input acceleration flight data are shown in Figs. A-25 through A-30 of Vol. II. Selected forcing functions $\{f(t)\}$ and their Fourier transforms $\{F(\omega)\}$ are shown in Figs. A-31 through A-33 of Vol. II. Because the OAO model, including its adaptor was too crude, the resulting forcing functions $\{f(t)\}$ have been found to be not satisfactory, exhibiting some unrealistic oscillations at about 60 Hz, as shown in Figs. A-31 through A-33.

D. ATS/Centaur Composite Vehicle

The composite analysis using the ATS model was performed by obtaining the normal modes of the ATS model cantilevered at gridpoint 23 of Fig. 9. Similarly to the previous cases, the appropriate $[M_{rr}]$, $[M_{er}]$ and $[\omega_n]$ matrices were generated to attach the ATS model to the Centaur model at gridpoint 12 of Fig. 5 and obtain the overall free-free Spacecraft/Vehicle modes. The modal data are shown in Tables 19, 20 and 21. Again, frequency

domain computations similar to section B were performed using the modal data and a modal damping $\zeta_n = .03$ for all modes. The time histories and the Fourier transforms of three sets of the input acceleration flight data, AC-17 MECO I, AC-18 MECO I and AC-18 MECO II, are shown in Figs. A-34 through A-51. Here again the ATS model was too crude to give acceptable results of the forcing function, therefore, only selected forcing functions $\{f(t)\}$ and their Fourier transforms obtained as for the previous cases are shown in Figs. A-52 through A-54 of Vol. II for AC-18 MECO II.

V. DISCUSSION

The accuracy of the method presented here for deriving forcing functions from measured responses depends, at the outset, on obtaining, from telemetry, phase coherent data with a minimum of electrical noise. The steps described in Ref. 1 to obtain phase coherent data are considered minimal. In any similar future application, on-board data processing leading to the desired acceleration components for direct telemetering should produce an improvement in signal quality.

The method is inherently sensitive to the fidelity in structural modeling, and, to a lesser degree, on the assumptions of modal damping in deriving the structural transfer matrices $[H(\omega)]$. For example, if the Fourier transform $\{A(\omega)\}$ of the acceleration vector $\{a(t)\}$ shows a dominant frequency component well removed from any computed normal-mode frequency of the space vehicle, the derived Fourier transform $\{F(\omega)\}$ will have an exaggerated amplitude at this frequency. Another way of saying this is that "ring out" due to a step forcing function can occur only in normal modes. A mismatch of computed modal frequencies with observed frequency response will cause a spurious "ring in" to the functions, $\{f(t)\}$, derived from this inverse process.

Modal data obtained from or confirmed by modal surveys would be highly desirable, as would, of course, direct measurements of the desired transfer functions [H(ω)]. However, the latter would require tests of the particular booster spacecraft combination, whereas mode surveys could be conducted independently for booster and spacecraft, and combined by modal synthesis techniques.

On several channels of the processed flight data, DC offsets were observed. These offsets led to derived increments of engine side force that could be obtained only with more than full gimbal angle. The origin of this inconsistency is thought to be electrical.

During each of the flights discussed herein, Centaur engine chamber pressure measurements were obtained through continuous telemetry channels. It was initially intended to compare the derived forcing functions with those converted from pressure measurements. However, subsequent investigations revealed that the response of the pressure sensing instrumentation was seriously degraded above 8Hz. Accordingly, no comparisons are available.

Early approaches to the "inverse solution" in the time domain revealed instabilities which are circumvented by operating in the frequency domain. Ref. 3 explains the reasons therefor.

The solution in the frequency domain is made practical through the use of the "fast Fourier transform" algorithm.

VI. CONCLUSION

To conclude, the numerical analysis performed on six flight events has shown that it is feasible to work backward from a known flight response to determine the dynamic load (forcing functions) at specific events. However, the method of analysis is successful only if the dynamic model of the entire structure is well known and the source of the loading is fully understood.

REFERENCES

1. Trubert, M. R., "Mariner 6 and 7 Low Frequency Flight Accelerations Measurement," Report PD 605-236, Jet Propulsion Laboratory, February 16, 1970, revised June 1971.

2. Trubert, M. R., Chisholm, J. R., and Gayman, W. H., "Use of Derived Forcing Functions at Centaur Main Engine Cutoff in Predicting Transient Loads on Mariner Mars '71 and Viking Spacecraft," Technical Memorandum 33-486, Jet Propulsion Laboratory, Pasadena, Calif. (in process).

3. Trubert, M. R., "A Fourier Transform Technique for the Prediction of Torsional Transients for a Spacecraft from Flight Data of Another Spacecraft Using the Same Booster," Technical Memorandum No. 33-350. Jet Propulsion Laboratory, October 15, 1967.

4. Trubert, M. R., "A Frequency Domain Solution for the Linear Attitude Control Problem of Spacecraft with Flexible Appendages," Technical Report 32-1478, Jet Propulsion Laboratory, November 15, 1970.

5. Hurty, W. C., "Dynamics of Structural Systems by Component Mode Synthesis," Technical Report No. 32-530, Jet Propulsion Laboratory, January 15, 1964.

6. Gieseke, R. K., "Input Data for Normal Mode Analysis," Report No. GDC-BT D69-002, General Dynamics Convair, January 27, 1969, revised April 1969.

7. Garba, J. A., Gayman, W. H., and Wada, B. K., "Computation of Torsional Vibration Modes of Ranger and Surveyor Space Vehicles," Technical Memorandum 33-277, Jet Propulsion Laboratory, April 1, 1968.

8. Lang, T. E., "Summary of the Functions and Capabilities of the Structural Analysis and Matrix Interpretive System Computer Program," Technical Report 32-1075, Jet Propulsion Laboratory, April 1, 1967.

9. Simpson, R. and Kruck, R., "Receptance Coupling Program (RECEP)" Doc. No. 900-442, Jet Propulsion Laboratory, March 30, 1971.

10. Bamford, R. M., Wada, B. K., Garba, J. A., and Chisholm, J. R., "Dynamic Analysis of Large Structural Systems" to be presented at the 1971 Winter Annual Meeting of ASME, Washington, D. C., November 2, 1971.

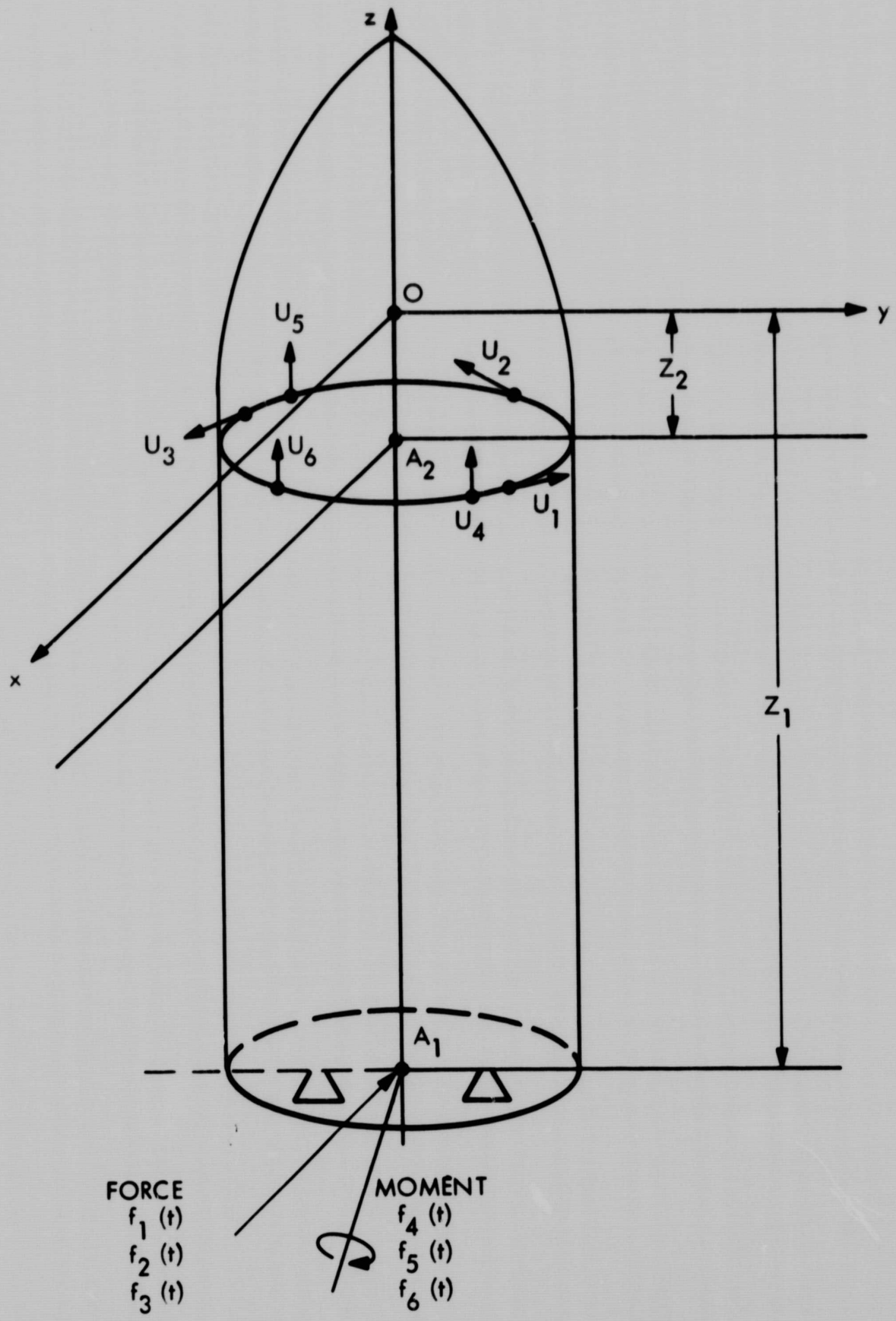

Fig. 1. Flight vehicle

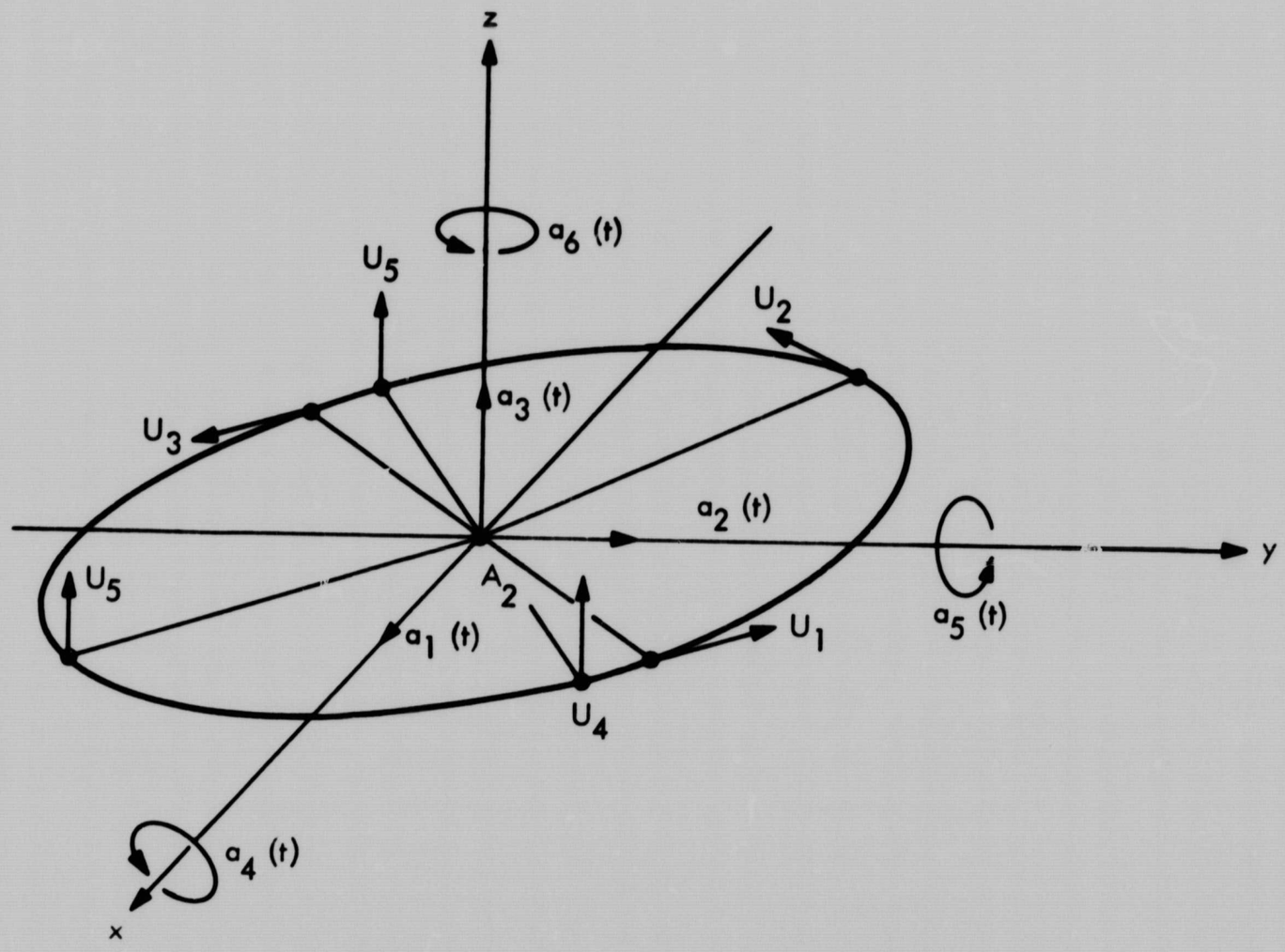

Fig. 2. Field joint motion

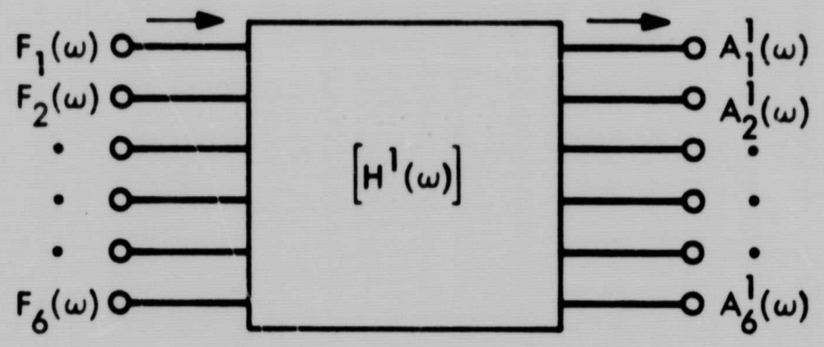

Fig. 3. Block diagram for force-response relationship

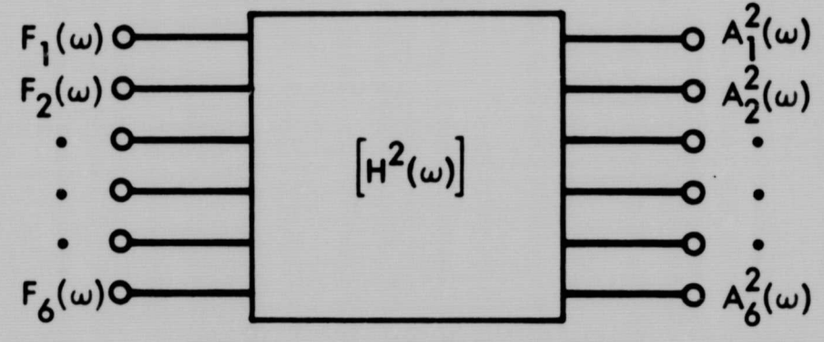

Fig. 4. Response of spacecraft on launch vehicle

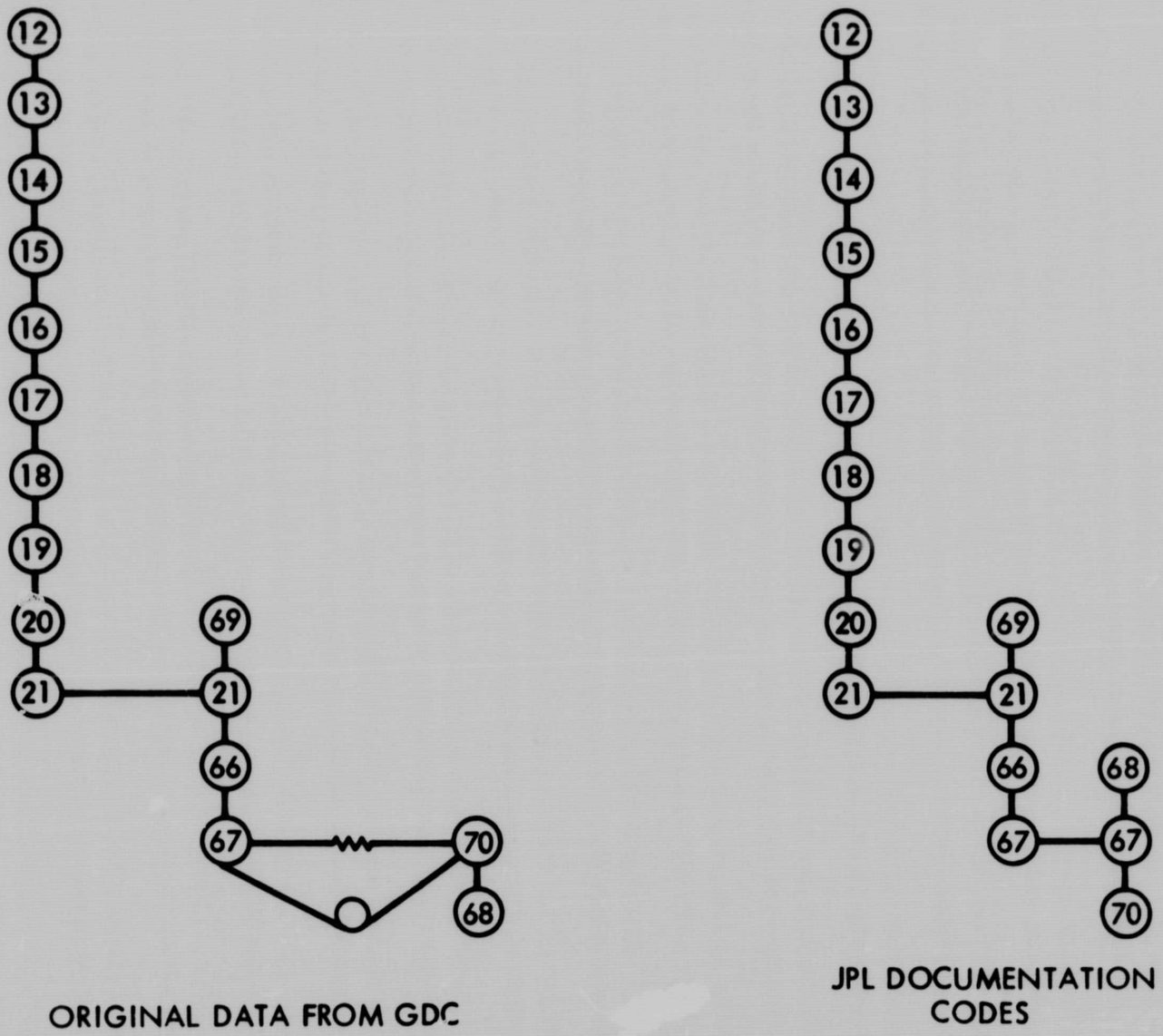

Fig. 5. Lateral model of the Centaur launch vehicle

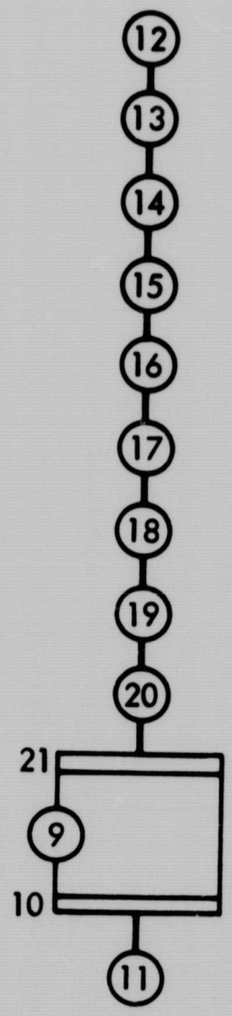

Fig. 6. GDC and JPL longitudinal model Centaur launch vehicle

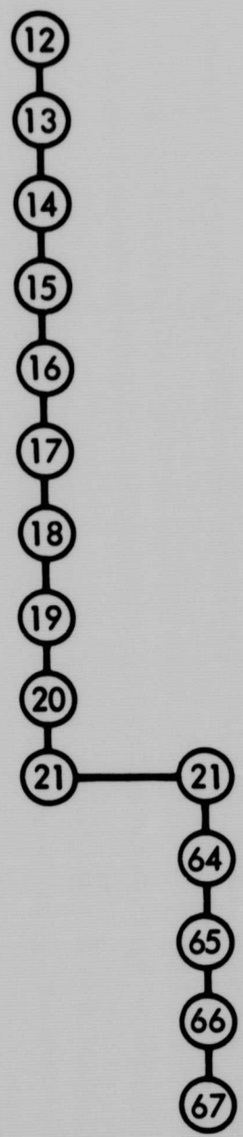

Fig. 7. GDC and JPL torsional model Centaur launch vehicle

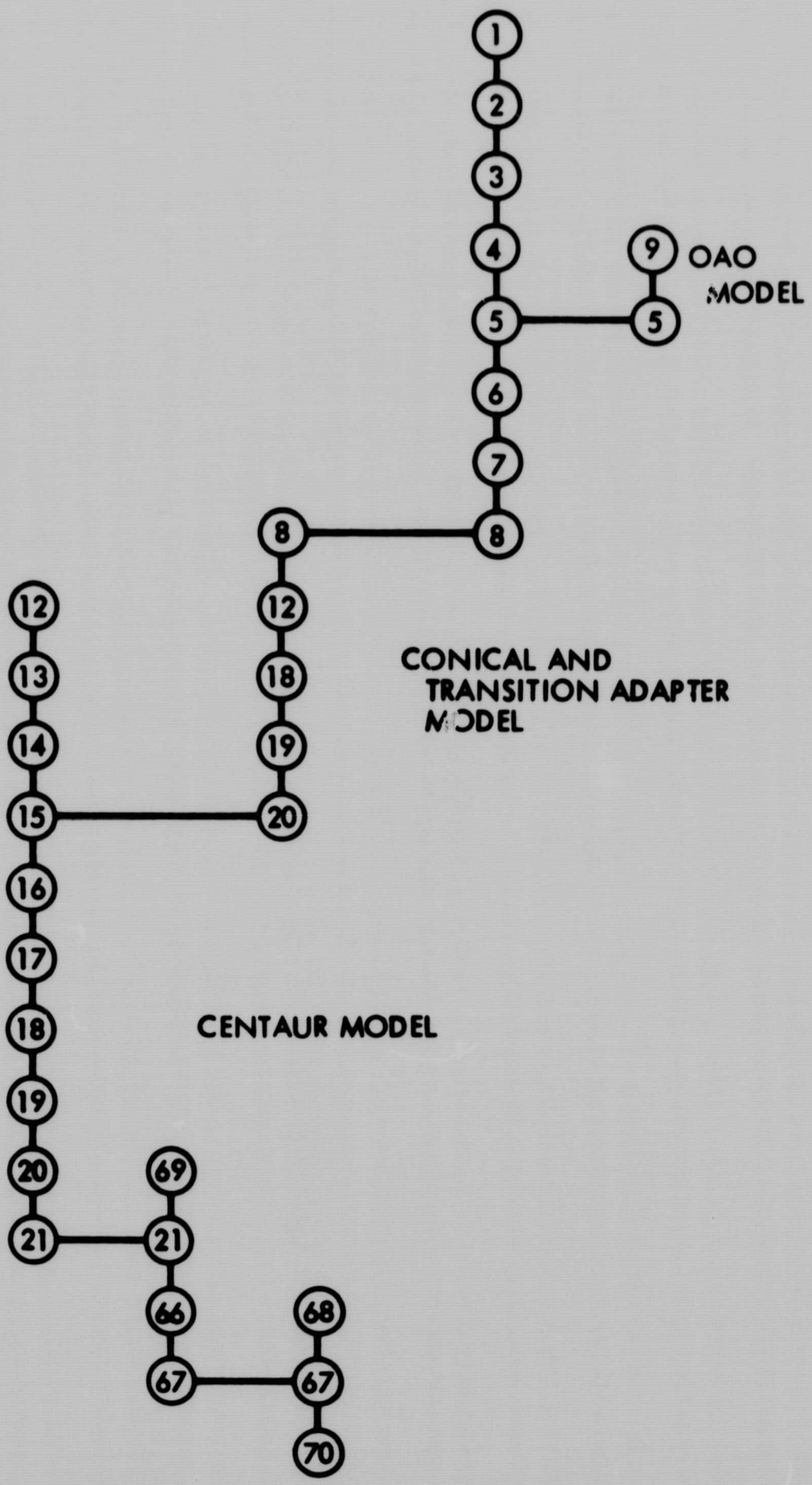

Fig. 8. OAO/Centaur model

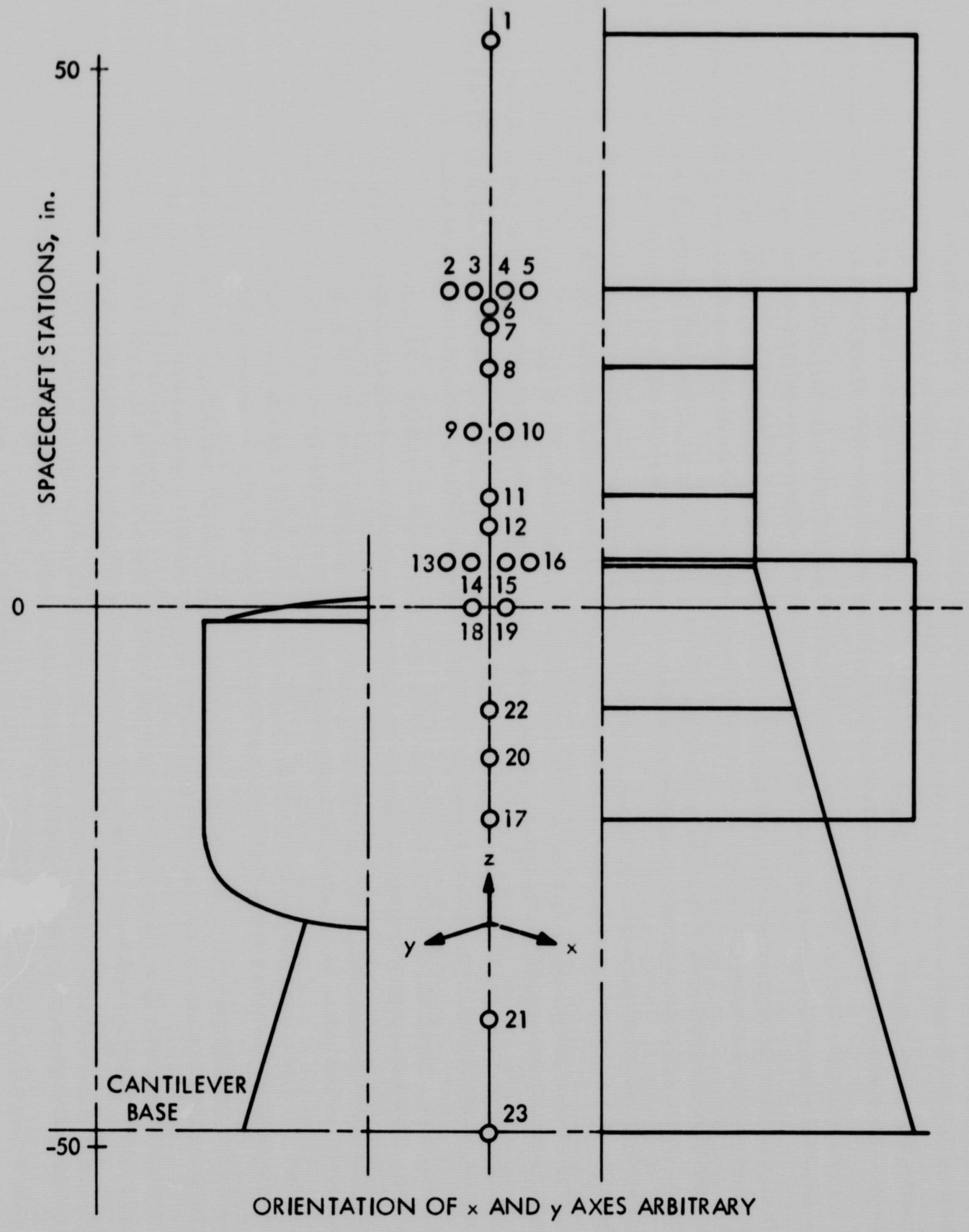

Fig. 9. ATS model

Table 1. Centaur MECO Torsional Model – Gridpoints, Station Locations, and Inertias

Gridpoint	Station (in.)	Inertia ($lb\text{-}in.^2$)
12	122.0	0.1551 E7
13	141.0	0.1247 E6
14	149.0	0.1551 E6
15	168.0	0.5930 E6
16	199.3	0.2291 E6
17	229.3	0.2499 E6
18	264.0	0.2758 E6
19	294.0	0.4164 E6
20	324.0	0.7243 E6
21	361.0	0.3665 E6
64	369.0	0.2546 E6
65	389.0	0.7525 E6
66	409.0	0.7551 E6
67	433.5	0.1224 E6

Table 2. Centaur MECO Lateral Model – Gridpoints, Station Locations, Weights, and Inertias

Gridpoint	Station (in.)	Weight (lb)	Inertia (lb-in.^{2})	
			Ix	Iy
12	122.0	921.0	0.7794 E6	0.7794 E6
13	141.0	277.0	0.6236 E5	0.6236 E6
14	149.0	79.0	0.7755 E5	0.7755 E5
15	168.0	171.0	0.2965 E6	0.2965 E6
16	199.3	93.0	0.1150 E6	0.1150 E6
17	229.3	93.0	0.1250 E6	0.1250 E6
18	264.0	91.0	0.1379 E6	0.1379 E6
19	294.0	91.0	0.2082 E6	0.2082 E6
20	324.0	273.0	0.3080 E6	0.3080 E6
21	361.0	507.0	0.1695 E6	0.6765 E6
66	387.0	270.0	0.2542 E6	0.2603 E6
67	403.0	561.0	0.9006 E6	0.4509 E6
68	398.9	197.7	-	-
69	337.0	-	-	-
70	437.2	524.4	-	-

Table 3. Centaur MECO Longitudinal Model – Gridpoints, Station Locations, and Weights

Gridpoint	Station (in.)	Weight (lb)
9	-	-
10	-	819.0
11	-	754.0
12	122.0	921.0
13	141.0	277.0
14	149.0	79.0
15	168.0	171.0
16	199.3	93.0
17	229.3	93.0
18	264.0	91.0
19	294.0	91.0
20	324.0	273.0
21	361.0	507.0

Table 4. Centaur MECO Lateral Model – Spring Constants

Gridpoint 1	Gridpoint 2	Stiffness (Pitch and Yaw)			
		EI_1 (10^{12} lb-in.^{2})	EI_2 (10^{12} lb-in.^{2})	KAG_1 (10^8-lb)	KAG_2 (10^8 lb)
12	13	0.055	0.203	0.122	0.221
13	14	0.0818	0.122	0.221	0.238
14	15	0.122	0.214	0.238	0.264
15	16	0.312	0.312	0.335	0.335
16	17	0.312	0.312	0.335	0.335
17	18	0.312	0.312	0.335	0.335
18	19	0.312	0.312	0.335	0.335
19	20	0.312	0.312	0.335	0.335
20	21	0.312	0.312	0.335	0.335
21	69	0.384	0.179	0.423	0.254
21	66	0.384	0.131	0.423	0.338
66	67	0.131	0.217	0.338	0.198
67	68	0.000000305	0.00000059	–	–
67	70	0.0001904	0.0001838	–	–

Table 5. Centaur MECO Longitudinal Model – Spring Constants

Gridpoint 1	Gridpoint 2	Stiffness K (10^6 lb/in.)
12	13	100.0
13	14	100.0
14	15	0.50
15	16	4.57
16	17	4.72
17	18	4.05
18	19	4.72
19	20	4.72
20	21	3.83
21	9	8.91
21	10	-0.33
9	10	0.61
10	11	20.0

Table 6. Centaur MECO Torsional Model — Spring Constants

Gridpoint 1	Gridpoint 2	Stiffness K 10^{10} in.-lb/rad
12	13	0.3672
13	14	0.8292
14	15	0.7290
15	16	0.6169
16	17	0.6374
17	18	0.5464
18	19	0.6169
19	20	0.6169
20	21	0.5168
21	64	3.168
64	65	0.8496
65	66	0.1296
66	67	0.00082

Table 7. Rigid Body Weight Matrix $|M_{RR}|$ for the Mariner '69 Spacecraft (Units: lb, in., sec)

	X	Y	Z	θ_x	θ_y	θ_z
X	0.89567+03	0.00000	0.00000	0.00000	-0.11012+05	-0.41730+03
Y	0.00000	0.89567+03	0.00000	0.11012+05	0.00000	0.38640+03
Z	0.00000	0.00000	0.89567+03	0.41730+03	-0.38640+03	0.00000
θ_x	0.00000	0.11012+05	0.41730+03	0.94243+06	0.36476+04	0.14680+03
θ_y	-0.11012+05	0.00000	-0.38640+03	0.36476+04	0.93547+06	-0.15842+05
θ_z	-0.41730+03	0.38640+03	0.00000	0.14680+03	-0.15842+05	0.51507+06

Table 8. Generalized Elastic-Rigid Coupling Terms $[M_{ER}]$ for the Mariner Mars '69 Spacecraft

(Units: lb, in., sec)

Frequency (Hz)	X	Y	Z	θ_x	θ_y	θ_z
6.445	0.78034-01	0.77060-01	-0.28800-03	0.64585+01	-0.58511+01	-0.86465+00
7.211	0.32283+00	-0.23007+00	0.18330-02	-0.15961+02	-0.22762+02	-0.11485+00
7.232	-0.22085+00	-0.31572+00	-0.60400-03	-0.22503+02	0.15749+02	-0.35514-01
7.522	0.26200-03	0.23000-03	0.41700-05	0.44100-03	-0.28419-01	0.37420-02
7.603	0.11400-03	-0.80000-04	-0.38090-01	-0.85170-02	-0.65740-02	0.90901-01
9.225	-0.76930-01	0.76460-01	-0.48216-02	0.65655+01	0.69361+01	-0.17988+01
18.811	-0.76100-02	-0.95000-03	0.81500-03	0.14724+00	0.26049+00	-0.16542-01
20.641	0.14412+00	0.48680-01	0.78520-02	0.24166+01	-0.65497+01	-0.13341+00
20.660	-0.77130-01	0.15861+00	0.42700-03	0.65854+01	0.30193+01	0.39951+00
22.145	0.79700-02	-0.12040-01	0.79200-03	-0.24058+00	-0.19051+00	-0.25326+01
27.354	0.59641+00	-0.68297+00	0.14590-01	-0.11437+02	-0.12243+02	-0.36408+01
27.727	0.26147+00	0.19671+00	-0.76800-03	0.17732+01	-0.20654+01	0.28'00-03
27.854	-0.15400-02	0.51130-02	-0.24500-03	0.67569-01	-0.86990-01	-0.79394-01
27.968	-0.98000-03	0.96000-03	0.24910-02	0.19697-01	0.29029-01	-0.59180-01
28.184	0.44499+00	-0.44172+00	0.16040-01	-0.11125+02	-0.12561+02	-0.33727+01
30.606	-0.77378+00	-0.78516+00	-0.12950-01	-0.18057+02	0.17237+02	-0.49332+00
35.727	-0.12097+00	0.97620-01	0.15880-01	0.52202+01	0.32425+01	-0.92349+01
36.174	-0.12976+00	0.68360-01	0.43010-02	0.20900+01	0.39941+01	-0.78517+01
40.792	0.76522+00	0.13723+00	-0.64230-01	-0.33988+01	0.11572+02	-0.10528+00
41.988	0.12887+00	-0.78379+00	-0.44790-01	0.10485+02	0.38013+01	-0.30819+00
51.498	-0.31573+00	0.28126-01	-0.13281+00	-0.12352+01	0.71127+01	0.13817+01
53.287	-0.15820+00	-0.28840-01	-0.57890-01	0.54186+00	0.19922+01	0.82660-02
58.260	0.48900-02	0.50600-02	0.56500-03	0.45048+00	0.44806+00	-0.25489+00
58.650	-0.51680-01	0.18240-01	0.62500-02	-0.18627+01	-0.34481+00	0.21881+01
59.359	-0.11200-01	-0.40460-01	0.22670-01	0.16875+01	0.49254+00	-0.39955+00
59.508	-0.80810-01	-0.15500-02	0.73960-02	-0.86114+00	-0.18632-01	0.73935+00
60.332	0.42660-02	-0.89100-02	-0.77990-02	-0.11639+00	0.41071-01	0.78316+00
68.010	0.51147-01	0.12267+00	-0.31114+00	0.87804+01	-0.10189+01	-0.43655+01
71.283	-0.48910-01	0.17100-01	-0.55926+00	-0.23008+01	-0.41685+01	0.11802+02
75.812	0.12456-01	0.31000-03	-0.31690-01	-0.38898+00	0.19092+00	-0.25818+01
75.995	0.23600-01	0.12890-01	-0.93650-01	-0.22196+01	-0.31010-01	-0.46249+01
76.079	0.56900-02	0.15450-01	-0.10717+00	-0.14906+01	-0.30123+00	-0.27620+01
76.195	-0.38740-01	-0.61800-02	0.69710-01	0.30601+00	0.54470-01	0.67510+00
77.970	0.43590-01	-0.48630-01	-0.28750+00	-0.83622+01	-0.14018+00	-0.16987+02
86.443	0.12802+00	-0.13533+00	-0.33050-01	-0.41984+01	-0.16655+01	0.21645+02
97.825	0.23378-01	-0.31780-01	-0.56250-01	-0.21877+01	-0.24365+00	-0.50806+00
104.958	0.35580-01	-0.15590-01	-0.19680-01	-0.10729+01	0.77540+00	-0.73696+00
106.205	-0.27970-02	0.49380-01	0.35770-01	0.23165+00	0.69936+00	0.17571+00
106.551	0.34500-01	0.11660-01	-0.64910-02	0.69390-01	0.15100+01	-0.62534+00
107.768	0.68600-03	-0.19200-02	-0.46490-02	0.81420-01	-0.28650-01	0.10117+00

Table 9. OAO Weight and Inertia Data

Gridpoint	GAEC Station	WT(x)(lb)	WT(y)(lb)	WT(z)(lb)	I(xx) ($\times 10^5$ lb-in.^{2})	I(yy) ($\times 10^5$ lb-in.^{2})	I(zz) ($\times 10^5$ lb-in.^{2})
1	44.5	237.6	237.6	327.6	1.634	2.498	2.827
2	61.0	346.4	346.4	398.4	2.728	2.460	5.361
3	81.0	780.5	780.5	728.5	4.063	3.634	9.332
4	100.0	746.7	746.7	717.7	4.526	3.132	8.389
5	119.0	778.7	778.7	721.3	4.551	3.360	9.727
6	139.0	391.0	391.0	477.4	3.260	2.959	5.871
7	155.5	439.9	439.9	349.9	2.294	2.342	5.684
8	174.0	88.0	88.0	88.0	0.370	0.370	0.740
9	98.0	831.1	831.1	831.1	6.280	6.280	1.720
Weights and inertias for reduced structural model for OAO A-II							
Total Weight 4640 lb							

Table 10. OAO Model Compliance Data

Grid-point A	Grid-point B	Length (in.)	Compliances of Elements ($\times 10^{-7}$)			
			Axial $\frac{L}{AE}$	Torsion $\frac{L}{JG}$	Bending $\frac{L}{3EI}$	Shear $\frac{K}{GAL}$
1	2	16.5	1.98	0.0197	0.00210	0.0941
2	3	20.0	2.32	0.0236	0.00244	0.0820
3	4	19.0	2.10	0.0222	0.00217	0.0803
4	5	19.0	1.82	0.0163	0.00186	0.0659
5	6	20.0	1.33	0.0096	0.00133	0.0483
6	7	16.5	9.58	0.0320	0.00601	0.0533
7	8	18.5	3.64	0.0521	0.00460	0.1000
5	9	43.0	43.0	0.0	0.0808	0.0

L = Length (in.)

A = Area ($in.^2$)

G = Shear Modulus ($lb/in.^2$)

J = Polar Moment of Inertia ($in.^4$)

I = Area Moment of Inertia ($in.^4$)

E = Young's Modulus ($lb/in.^2$)

K = Shear Factor

Table 11. ATS Model Stiffness Data

Grid-point A	Grid-point B	Stiffness K_{AB} Between Gridpoint A and Gridpoint B (lb/in.)					
		X	Y	Z	θ_X	θ_Y	θ_Z
1	2	0.334 E6	0.258 E5	0.258 E5	0.401 E8	0.1089 E9	0.1089 E9
3	4	0.7996 E5	0.12 E7	0.168 E7	0.1098 E10	0.116 E9	0.1390 E8
4	5	0.216 E5	0.216 E5	0.216 E5	0.5661 E7	0.2831 E7	0.2831 E7
6	7	0.504 E5	0.504 E5	0.504 E5	0.1662 E8	0.8047 E7	0.8047 E7
7	8	0.504 E5	0.504 E5	0.504 E5	0.1662 E8	0.8047 E7	0.8047 E7
10	11	0.605 E5	0.6055 E5	0.6055 E5	0.8181 E7	0.3001 E7	0.3001 E7
11	12	0.172 E5	0.1718 E5	0.1718 E5	0.144 E7	0.5826 E6	0.5826 E6
12	13	0.172 E5	0.1718 E5	0.1718 E5	0.144 E7	0.5826 E6	0.5826 E6
13	14	0.996 E6	0.2 E9	0.2 E9	0.121 E9	0.908 E8	0.908 E8
14	15	0.323 E5	0.12 E7	0.12 E7	0.988 E8	0.173 E8	0.173 E8
15	16	0.65 E6	0.2 E9	0.2 E9	0.31 E9	0.2325 E9	0.2325 E9
16	17	0.334 E6	0.258 E5	0.258 E5	0.401 E8	0.1089 E9	0.1089 E9
18	19	0.2 E9	0.2 E9	0.2 E9	0.2 E9	0.244 E10	0.244 E10
19	20	0.153 E7	0.6725 E6	0.6725 E5	0.217 E9	0.3183 E9	0.3183 E9
20	21	0.2 E9	0.15 E5	0.15 E5	0.2 E9	0.2 E9	0.2 E9
22	23	0.47 E7	0.471 E6	0.471 E6	0.435 E9	0.356 E9	0.356 E9
2	4	0.65 E6	0.2 E9	0.2 E9	0.31 E9	0.2325 E9	0.2325 E9
3	6	0.996 E6	0.2 E9	0.2 E9	0.121 E9	0.908 E8	0.908 E8
6	8	0.271 E7	0.908 E6	0.908 E6	0.2 E9	0.4448 E9	0.4448 E9
8	11	0.248 E7	0.484 E6	0.484 E6	0.1085 E9	0.2292 E9	0.2292 E9
11	13	0.372 E7	0.736 E6	0.736 E6	0.1625 E9	0.3564 E9	0.3564 E9
13	18	0.78 E8	0.6151 E7	0.6151 E7	0.248 E10	0.2733 E10	0.2733 E10
18	22	0.1365 E7	0.159 E7	0.159 E7	0.695 E9	0.755 E9	0.755 E9
8	10	0.605 E5	0.6055 E5	0.6055 E5	0.8181 E7	0.3001 E7	0.3001 E7
9	15	0.447 E5	0.4471 E5	0.4471 E5	0.2251 E8	0.7334 E7	0.7334 E7
4	9	0.447 E5	0.4471 E5	0.4471 E5	0.2251 E8	0.7334 E7	0.7334 E7
3	5	0.216 E5	0.216 E5	0.216 E5	0.5661 E7	0.2831 E7	0.2831 E7
4	15	0.41 E6				0.144 E9	0.144 E9

Table 12. ATS. Coordinate, Weight and Inertia Data (Units: lb, in., sec)

Station No.	Z Coordinate	Inertia					
		X	Y	Z	θ_x	θ_y	θ_z
1	0.525 E01	0.2082 E02	0.2082 E02	0.2082 E02	0.815 E04	0.815 E04	0.1630 E05
2	0.305 E02	0.1772 E02	0.1772 E02	0.1772 E02	0.6950 E04	0.6950 E04	0.1390 E05
3	0.305 E02	0.1168 E02	0.1168 E02	0.1168 E02	0.1150 E04	0.1150 E04	0.2300 E04
4	0.305 E02	0.1836 E02	0.1836 E02	0.1836 E02	0.7200 E04	0.7200 E04	0.1440 E05
5	0.305 E02	0.1068 E02	0.1068 E02	0.1068 E02	0.1050 E04	0.1050 E04	0.2100 E04
6	0.226 E02	0.6600 E02	0.6600 E02	0.6600 E02	0.8650 E04	0.8650 E04	0.1730 E05
7	0.265 E02	0.1540 E03	0.1540 E03	0.1540 E02	0.2540 E05	0.2540 E05	0.5080 E05
8	0.225 E02	0.1678 E02	0.1678 E02	0.1678 E02	0.1650 E04	0.1650 E04	0.3300 E04
9	0.165 E02	0.1366 E03	0.1366 E03	0.1366 E03	0.3440 E05	0.3440 E05	0.6880 E05
10	0.165 E02	0.1850 E03	0.1850 E03	0.1850 E03	0.1250 E05	0.1250 E05	0.2500 E05
11	0.105 E02	0.1645 E02	0.1645 E02	0.1645 E02	0.1600 E04	0.1600 E04	0.3200 E04
12	0.650 E01	0.5250 E02	0.5250 E02	0.5250 E02	0.2200 E04	0.2200 E04	0.4400 E04
13	0.250 E01	0.1865 E02	0.1865 E02	0.1865 E02	0.1850 E04	0.1850 E04	0.3700 E04
14	0.250 E01	0.1100 E02	0.1100 E02	0.1100 E02	0.1100 E04	0.1100 E04	0.2200 E04
15	0.250 E02	0.1665 E02	0.1665 E02	0.1665 E02	0.6550 E04	0.6550 E04	0.1310 E05
16	0.250 E01	0.1614 E02	0.1614 E02	0.1614 E02	0.6350 E04	0.6350 E04	0.1270 E05
17	-0.195 E02	0.2437 E02	0.2437 E02	0.2437 E02	0.9550 E04	0.9550 E04	0.1910 E05
18	0	0.2317 E02	0.2317 E02	0.2317 E02	0.2250 E04	0.2250 E04	0.4500 E04
19	0	0	0	0	0.4200 E04	0.4200 E04	0
20	-0.110 E02	0.80224 E03	0.80224 E03	0.84205 E03	0.4000 E05	0.4000 E05	0.8840 E05
21	-0.330 E02	0.3981 E02	0.3981 E02	0	0	0	0
22	-0.900 E01	0.5148 E02	0.5148 E02	0.5148 E02	0.7450 E04	0.7450 E04	0.1490 E05
23	-0.488 E02	-0.3380 E02	-0.3380 E02	-0.3380 E02	-0.1325 E05	-0.1325 E05	-0.2650 E05

Table 13. ϕ_{lr} and ϕ_{le} for MECO Centaur/Mariner Mars '69 Model (Units: lb, in., sec)

	f (Hz)	X	Y	Z	θ_x	θ_y	θ_z
ϕ_{lr}	0 0 0 0 0 0	1.0	1.0	1.0	1.0	1.0	1.0
ϕ_{le}	6.1454	0.5039-06	-0.5434-06	-0.2727-07	-0.9328-08	-0.9049-08	-0.5932-08
	7.2115	0.1978-05	0.1360-05	-0.9688-07	0.2603-07	-0.3686-07	0.3685-08
	7.2325	0.1358-05	-0.1912-05	-0.5854-07	-0.3605-07	-0.2527-07	-0.5276-09
	7.5227	0.3511-08	-0.4357-09	-0.3223-09	-0.4537-10	-0.3828-10	0.2912-10
	7.603	0.1016-07	0.7269-10	-0.3876-06	0.4349-10	-0.7632-10	0.6378-09
	9.2257	-0.5612-06	-0.4861-06	-0.1990-07	-0.9331-08	0.9691-08	-0.1379-07
	15.947	0.8785-05	0.1169-04	-0.7966-06	0.2063-08	-0.3150-06	0.6302-04
	18.577	-0.9081-04	-0.1252-01	0.1675-04	-0.3525-04	0.1966-06	0.9818-05
	18.791	0.8076-06	-0.2175-06	0.3868-08	-0.5640-09	-0.1476-08	0.4031-09
	18.992	-0.1182-01	0.1246-03	0.1142-03	0.3821-06	0.3208-04	-0.6124-05
	20.642	-0.3235-05	0.1085-05	-0.3170-07	0.8004-08	0.2320-07	-0.1377-08
	20.66	-0.1558-05	-0.3129-05	0.3998-07	-0.2437-07	0.1178-07	0.2575-08
	22.145	-0.8857-08	-0.1940-06	-0.6988-08	-0.1714-08	0.6929-09	0.2202-07
	27.355	0.3061-05	0.4301-05	0.6997-07	0.7759-07	-0.6647-07	-0.2478-07
	27.727	-0.9014-06	0.9583-06	0.5035-07	0.2080-07	0.2624-07	-0.3069-09
	27.855	0.6256-08	-0.2591-07	-0.2976-08	-0.5564-09	0.1744-10	-0.6921-09
	27.968	0.8487-08	0.5363-08	-0.2908-07	0.9216-10	-0.1884-09	0.5323-09
	28.185	-0.2346-05	-0.3324-05	-0.1323-06	-0.5460-07	0.5254-07	0.2557-07
	30.606	0.1494-06	0.5113-05	-0.1116-06	0.9786-07	0.8221-07	-0.3688-08
	32.447	0.8885-02	-0.1632-04	-0.5888-04	-0.1581-06	-0.2085-04	0.2091-05
	35.727	0.1696-05	0.1855-05	-0.3746-06	0.2726-07	-0.1525-07	0.2204-06
	35.789	0.4810-04	-0.1219-03	-0.1136-05	-0.1171-05	-0.4262-06	-0.1031-04
	36.175	-0.2450-05	0.2500-10	0.1338-06	-0.6085-08	0.2280-07	-0.7636-07
	37.228	-0.1689-03	0.6226-05	-0.1411-02	-0.3272-06	0.1450-05	-0.1116-06
	38.957	0.3065-04	-0.7529-02	0.2438-05	-0.1150-04	-0.1376-06	0.1237-04
	40.792	0.7224-06	0.4910-06	-0.5238-06	-0.1051-07	-0.7164-07	0.2371-08
	41.989	-0.3857-06	0.1289-05	-0.4702-06	0.7850-07	-0.8295-08	0.1465-08
	51.5	0.4685-05	-0.2320-06	0.2391-05	0.9575-09	-0.7826-07	-0.2824-07
	53.288	-0.1935-05	0.6190-08	-0.1147-05	0.3477-08	0.3688-07	-0.5973-09
	58.262	0.2199-05	0.2535-06	0.6520-08	0.3314-08	-0.1627-08	0.8482-08
	58.652	-0.1766-06	0.4825-06	0.9744-07	0.1951-08	0.1014-07	0.8213-07
	59.36	0.4268-05	0.5488-06	-0.4493-06	0.9133-09	-0.5108-08	0.1527-07
	59.509	-0.7591-06	0.3979-06	0.4977-07	0.4509-08	0.1932-07	0.2950-07
	60.333	-0.5227-07	0.2927-07	0.1859-06	-0.1433-09	-0.1362-09	-0.3618-07
	68.011	0.3538-05	-0.1667-06	-0.1097-04	0.1593-07	-0.1033-06	-0.1826-05
	68.556	-0.9587-03	-0.5288-02	-0.6899-03	-0.9614-04	0.3357-04	0.5019-03
	71.285	-0.1164-04	-0.3652-04	0.2441-04	-0.6746-06	0.1752-06	0.1408-05
	72.651	-0.1477-01	0.3266-02	-0.7394-02	0.6476-04	0.2793-03	-0.3063-04
	74.038	0.2464-02	0.1478-01	0.2936-02	0.2861-03	-0.3939-04	0.2024-03
	75.814	0.2859-05	0.1523-05	-0.9593-06	0.2584-07	-0.4512-07	0.2066-06
	75.997	0.5432-05	-0.4328-05	-0.7600-05	-0.1038-06	-0.7744-07	0.2845-06
	76.08	-0.5345-05	0.2322-05	0.9663-05	0.5956-07	0.7116-07	-0.1758-06

Table 14. ϕ_{2r} and ϕ_{2e} for MECO Centaur/Mariner Mars '69 Model (Units: lb, in., sec)

	f (Hz)	X	Y	Z	θ_x	θ_y	θ_z
ϕ_{2r}	0	1.0					
	0		1.0		-281.0	281.0	
	0			1.0			
	0				1.0		
	0					1.0	
	0						1.0
ϕ_{2e}	6.4454	-0.1994-05	-0.2029-05	-0.2777-07	-0.8321-08	-0.8140-08	-0.5763-08
	7.2115	-0.8153-05	-0.5791-05	-0.1009-06	0.2289-07	-0.3241-07	0.3746-08
	7.2325	-0.5585-05	0.7981-05	-0.6111-07	-0.3157-07	-0.2217-07	-0.6660-09
	7.5227	-0.7600-08	0.4339-08	-0.3969-09	-0.1703-10	-0.3448-10	0.2306-10
	7.603	-0.1186-07	-0.3597-08	-0.3647-06	0.2891-10	-0.7563-10	0.6087-09
	9.2257	0.2054-05	0.2025-05	-0.1425-07	-0.7173-08	0.7462-08	-0.1294-07
	15.947	-0.3937-04	-0.1242-03	-0.8645-06	0.8105-06	-0.1669-06	0.8568-04
	18.577	0.1365-04	0.1998-02	0.1370-04	-0.5964-04	0.4432-06	0.8377-05
	18.791	0.3253-07	0.2488-07	-0.2166-08	-0.824[illegible]-09	-0.3617-08	0.5497-09
	18.992	0.1958-02	-0.6544-05	0.1345-03	0.4989-06	0.5704-04	-0.8211-05
	20.642	0.3777-05	-0.1279-05	0.2900-07	0.5748-08	0.1802-07	-0.1780-08
	20.66	0.1964-05	0.4029-05	0.4565-07	-0.1839-07	0.9418-08	0.7026-09
	22.145	0.1656-06	0.2471-06	-0.9288-09	-0.1181-08	0.3247-09	0.1531-07
	27.355	-0.1289-04	-0.1461-04	-0.2291-06	0.4324-07	-0.2891-07	-0.5703-08
	27.727	0.5352-05	-0.4069-05	0.7411-07	0.1471-07	0.1837-07	-.1195-08
	27.855	0.2362-07	0.1087-06	0.3320-08	-0.3567-09	0.3241-09	-0.4201-09
	27.968	-0.2227-07	-0.2167-07	0.5736-08	0.6137-10	-0.1862-10	0.2905-09
	28.185	0.9848-05	0.9745-05	0.2145-06	-0.1943-07	0.1105-07	0.7010-08
	30.606	0.1621-04	-0.1704-04	0.3659-06	-0.2535-07	-0.2793-08	0.9152-08
	32.447	-0.9553-03	-0.7724-05	-0.5118-04	0.7258-07	-0.5336-04	0.7064-05
	35.727	-0.2223-05	-0.1691-05	0.1492-05	-0.2219-07	-0.1192-08	-0.8337-06
	35.789	-0.5172-04	-0.7049-04	0.2873-05	0.8901-06	-0.5461-06	0.7886-04
	36.175	0.3099-05	0.1734-05	-0.5682-06	0.5436-09	0.5177-08	-0.1466-06
	37.228	0.4129-04	0.1707-04	0.1372-01	0.2167-05	-0.1983-05	-0.2962-06
	38.957	-0.9603-05	0.9540-03	0.1333-03	-0.5706-04	-0.2383-06	0.1211-04
	40.792	-0.1353-04	0.2235-05	-0.4746-05	-0.2934-07	-0.1339-06	-0.2167-08
	41.989	-0.2116-05	-0.1393-04	-0.2681-05	0.1381-06	-0.3361-07	0.1282-07
	51.5	-0.6243-05	-0.3461-06	0.3388-05	0.1610-07	0.4711-07	0.1258-07
	53.288	0.2929-05	-0.4574-06	-0.1356-05	0.8689-08	-0.1003-07	-0.4805-09
	58.262	0.4979-07	-0.1345-06	-0.5730-08	-0.7019-08	0.7900-08	-0.3696-08
	58.652	0.8371-06	0.2642-07	0.2050-06	-0.3047-07	0.7645-08	-0.4500-07
	59.36	-0.2392-06	0.5238-06	-0.4708-06	-0.3380-07	0.8280-08	-0.8685-08
	59.509	0.1324-05	-0.1300-06	0.2574-06	-0.1479-07	0.4317-08	-0.1663-07
	60.333	0.7906-07	0.2198-06	0.1[illegible]09-06	-0.1164-09	0.2132-08	0.2169-07
	68.011	-0.4162-06	0.5057-05	-0.4659-05	0.1683-06	0.1439-06	0.1507-05
	68.556	-0.3432-03	-0.1541-02	0.2083-03	0.8282-04	-0.3848-04	-0.4421-03
	71.285	-0.1583-05	-0.9506-05	0.5753-05	0.7351 06	-0.3814-06	-0.1428-05
	72.651	-0.4237-02	0.9232-03	0.2679-02	-0.5989-04	-0.3056-03	0.3996-04
	74.038	0.6526-03	0.3880-02	-0.8613-03	-0.3257-03	0.4386-04	-0.1230-03
	75.814	0.5315-06	0.2420-06	-0.4785-06	-0.5420-07	0.4723-07	-0.1953-06
	75.997	0.6910-06	-0.1739-05	0.1842-06	0.2200-07	0.1049-06	-0.3029-06
	76.08	-0.7857-06	0.9067-06	-0.5768-06	0.2920-09	-0.1201-06	0.1857-06

Table 15. Rigid Body Mass Matrix $[M_{rr}]$ for MECO Centaur/Mariner Mars '69 Model

	X	Y	Z	θ_x	θ_y	θ_z
X	0.13050+02	-0.49474-11	-0.26034-05	-0.50929-05	0.19177+04	-0.57657+01
Y	-0.49494-11	0.13053+02	0.12013-05	-0.19161+04	0.50863-05	0.17467+02
Z	-0.26028-05	0.12014-05	0.13102+02	5.7657	-17.467	0.00000
θ_x	-0.50929-05	-0.19161+04	+0.57657+01	0.51818+06	+ 0.95677+02	-0.23016+04
θ_y	0.19177+04	0.50865-05	-0.17467+02	0.95677+02	0.51828+06	0.10840+04
θ_z	-0.57657+01	0.17467+02	0.00000	-0.23016+04	0.10840+04	0.19209+05

Table 16. ϕ_{lr} and ϕ_{le} for MECO Centaur/OAO Model (Units: lb, in., sec)

	f (Hz)	X	Y	Z	θ_x	θ_y	θ_z
ϕ_{lr}	0	1.0					
	0		1.0				
	0			1.0			
	0				1.0		
	0					1.0	
	0						1.0
ϕ_{le}	17.080	0.2433-03	-0.5091-03	-0.1628-04	0.8613-05	0.8942-05	0.2931-03
	19.956	-0.3604-03	0.4063-02	0.4444-04	-0.1200-03	-0.5989-05	0.9270-04
	20.142	-0.4960-02	-0.5048-03	0.1245-03	0.8258-05	-0.9598-04	-0.4067-05
	20.909	-0.8996-04	0.1604-02	0.3115-05	0.3352-04	-0.1349-04	-0.2206-03
	22.746	-0.1854-02	0.1462-01	-0.2142-03	0.4785-03	0.6810-04	0.6698-04
	23.795	-0.1278-01	-0.2227-02	-0.4413-03	-0.8175-04	0.5170-03	-0.3761-04
	24.667	0.2343-03	-0.2049-02	-0.1878-04	0.8252-04	-0.4697-05	-0.2838-05
	24.794	-0.1235-02	-0.3363-03	-0.1860-03	-0.2330-04	0.2335-03	-0.2674-05
	31.412	0.2199-04	-0.2025-02	-0.1470-04	0.7983-04	-0.5254-05	-0.6566-05
	31.790	-0.2968-02	-0.9448-04	-0.4167-04	-0.6088-05	0.1643-03	-0.3322-05
	34.122	-0.1455-01	-0.6858-04	-0.3498-04	-0.6787-05	0.1279-03	-0.1609-04
	37.579	-0.1462-02	0.9579-04	-0.5223-06	-0.1479-04	0.1444-04	-0.2654-03
	40.233	-0.2328-03	-0.1243-01	-0.4000-05	-0.9845-04	0.6787-05	-0.3881-04
	42.245	-0.3597-03	-0.4252-03	-0.1817-03	0.2527-05	-0.1153-04	-0.2561-05
	49.139	0.1020-03	0.3955-03	0.4613-06	0.3421-05	-0.1586-05	0.5677-04
	50.283	0.3162-05	0.5963-03	0.4447-05	-0.1927-05	0.2984-06	-0.3748-05
	50.814	0.1190-02	0.3534-04	-0.7635-04	0.5325-06	0.2141-05	0.6709-05
	59.378	-0.1003-03	-0.8402-04	-0.5054-03	0.1915-05	-0.1476-05	-0.5408-06
	68.026	-0.7405-03	0.3544-03	-0.2978-01	0.1802-04	0.7856-04	0.1644-05
	79.644	0.3192-05	0.2273-02	0.8387-04	-0.4717-04	0.4246-06	0.2133-04
	80.577	-0.1318-02	0.2459-04	0.1133-02	0.1759-05	-0.6647-04	0.3829-05
	84.266	-0.2546-04	-0.1980-03	-0.2924-04	-0.1455-06	0.2061-05	-0.3021-04
	91.650	0.2844-03	0.2438-03	0.5149-02	-0.6646-05	-0.1878-04	0.1066-05
	97.336	-0.3157-03	0.1926-04	0.1350-03	0.1681-06	-0.1132-04	0.1377-05

Table 17. Φ_{2r} and Φ_{2e} for MECO Centaur/OAO Model (Units: lb. in., sec)

	f (Hz)	X	Y	Z	θ_x	θ_y	θ_z
Φ_{2r}	0	1.0				371.5	
	0		1.0		-371.5		
	0			1.0			
	0				1.0		
	0					1.0	
	0						1.0
Φ_{2e}	17.080	-0.8941-04	-0.6114-03	-0.3242-05	-0.1901-06	0.2045-06	0.3299-04
	19.956	-0.1042-02	0.1160-01	0.3787-04	-0.3789-04	-0.3345-05	-0.6135-04
	20.142	-0.1199-01	-0.1187-02	-0.1531-03	0.4150-05	0.3901-04	-0.9352-05
	20.909	-0.7986-03	0.2943-02	0.4419-05	-0.1306-04	-0.2342-05	0.2940-03
	22.746	0.1054-03	-0.2126-03	0.3473-06	0.4092-05	0.1203-05	-0.3672-04
	23.795	0.1870-03	0.1929-04	0.1736-04	-0.1693-05	0.1528-04	0.1406-04
	24.667	0.2268-03	-0.4475-02	-0.3244-04	-0.1302-04	-0.8828-06	-0.2329-04
	24.794	0.5034-02	0.2261-03	0.1095-03	0.2663-06	-0.8771-05	-0.2281-05
	31.412	0.5716-04	0.6842-02	-0.3915-04	-0.7101-04	0.4099-06	-0.1946-04
	31.790	-0.6721-02	0.4825-04	0.8030-04	-0.6000-06	-0.7027-04	-0.6691-05
	34.122	0.1214-02	-0.5578-05	-0.3314-04	0.8115-07	0.2305-04	0.4183-05
	37.579	-0.4789-04	-0.8697-05	0.1332-05	0.3214-06	0.9302-06	0.5467-04
	40.233	-0.4915-05	-0.7170-03	0.4856-04	0.4013-05	0.1701-06	0.1317-04
	42.245	-0.3915-03	-0.2127-03	-0.3140-02	0.2006-06	-0.1468-07	0.2015-06
	49.135	0.6022-03	-0.1092-02	-0.8552-06	0.3313-05	0.1397-05	0.3615-04
	50.283	-0.1278-03	-0.2363-01	0.6472-04	0.8625-04	-0.4196-06	0.4532-05
	50.814	-0.2380-01	0.1049-03	0.1054-03	-0.4090-06	-0.9509-04	-0.4100-05
	59.378	0.7739-04	0.5547-04	0.3138-02	-0.6273-07	0.2449-06	-0.9598-07
	68.026	0.5550-03	-0.4256-04	-0.6871-04	0.1193-05	0.1699-04	0.2855-06
	79.644	0.1174-03	-0.1225-01	0.6803-04	0.5185-03	0.5133-05	-0.1130-04
	80.577	0.1162-01	0.1297-03	0.5421-04	-0.5574-05	0.5181-03	-0.7587-05
	84.266	-0.1374-03	0.1877-03	0.1756-05	-0.1024-04	-0.7370-05	-0.2044-03
	91.650	0.1392-03	-0.1018-03	-0.8589-02	0.5785-05	0.8928-05	0.2672-06
	97.336	0.2715-02	-0.3231-05	-0.6818-04	0.7832-08	0.5181-04	-0.8348-06

Table 18. Rigid Body Mass Matrix $[M_{rr}]$ for MECO Centaur/OAO Model (Units: lb, in., sec)

	X	Y	Z	θ_x	θ_y	θ_z
X	0.26333+02	0.21764-11	- 0.32066-05	0.17923-05	0.76011+04	-0.68456+01
Y	0.23118-11	0.26336+02	0.53093-06	- 0.75996+04	- 0.75216-06	0.16467+02
Z	-0.32078-05	0.53093-06	0.26389+02	6.8456	-16.467	0.00000
θ_x	0.75471-06	-0.75996+04	6.8456	0.29990+07	0.10511+03	-0.20202+04
θ_y	0.76011+04	-0.17930-05	-16.467	105.11	0.29984+07	0.82157+03
θ_z	-0.68456+01	0.16467+02	0.00000	- 0.2022104	0.82158+03	0.30729+05

Table 19. ϕ_{lr} and ϕ_{le} for MECO Centaur/ATS Model (Units: lb, in., sec)

	f (Hz)	X	Y	Z	θ_x	θ_y	θ_z
ϕ_{lr}	0	1.0					
	0		1.0				
	0			1.0			
	0				1.0		
	0					1.0	
	0						1.0
ϕ_{le}	15.951	0.1103-04	0.2440-04	-0.2086-06	-0.2922-06	-0.2359-06	0.6374-04
	18.322	-0.8643-04	-0.1169-01	0.1840-04	-0.2257-04	0.1164-06	0.1078-04
	18.743	-0.1105-01	0.1217-03	0.4379-04	0.2885-06	0.1970-04	-0.5608-05
	31.821	-0.5702-02	0.1476-04	0.4461-04	0.9328-07	-0.1079-04	-0.1666-05
	33.268	-0.8417-04	-0.8260-04	-0.4917-02	-0.1456-05	-0.4438-06	-0.8027-07
	35.575	-0.3997-04	0.2736-02	-0.4369-04	0.6418-04	0.6090-06	0.7191-05
	35.742	-0.2385-03	-0.3191-03	0.7016-05	-0.9796-05	0.1822-05	0.1740-04
	36.690	0.8817-02	0.2325-06	-0.1476-04	-0.1803-06	-0.7236-04	-0.4714-05
	39.599	-0.6770-06	0.8845-02	0.1760-05	0.3206-04	-0.3087-07	-0.9501-05
	44.105	-0.1012-02	0.8738-03	-0.1512-05	0.7492-05	0.7887-05	-0.1545-03
	50.868	-0.8535-02	0.1182-02	-0.7245-04	0.1858-04	0.1339-05	0.1104-05
	51.065	-0.1159-02	-0.8801-02	-0.9592-04	-0.1356-03	0.1700-04	-0.4652-05
	54.416	-0.1824-03	-0.1740-04	0.5154-02	0.1050-05	0.3587-05	0.1850-06
	60.343	-0.3078-02	0.2280-04	-0.2635-04	0.6762-06	0.4961-04	0.6872-05
	60.471	-0.3209-04	-0.3198-02	-0.6449-04	-0.5280-04	0.5594-07	0.2318-05
	70.407	-0.3569-02	0.2378-03	0.2737-02	0.6263-05	0.7051-04	0.2306-04
	70.492	-0.1185-03	-0.3273-02	-0.7684-02	-0.6857-04	-0.1326-05	0.3971-04
	70.747	-0.1031-03	-0.1362-02	0.1737-01	-0.2172-04	0.1189-04	0.2465-04
	70.829	0.3646-03	0.4720-03	-0.2242-02	0.8900-05	-0.6059-05	0.5455-04
	74.051	-0.5396-03	0.1110-02	0.7349-04	0.2389-04	-0.7723-04	-0.5251-03
	89.907	-0.9306-02	0.1135-01	0.1490-02	0.3024-03	0.2269-03	0.6849-04
	90.807	0.1226-01	0.9272-02	-0.3688-04	0.2428-03	-0.2775-03	0.8058-04
	93.490	-0.1636-02	0.1862-02	-0.1633-01	0.4462-04	0.1562-04	0.9906-05
	136.36	-0.3619-03	0.5043-02	-0.1359-03	0.4638-03	0.5339-04	0.5255-04

Table 20. Φ_{2r} and Φ_{2e} for MECO Centaur/ATS Model (Units: lb. in., sec)

	f (Hz)	X	Y	Z	θ_x	θ_y	θ_z
Φ_{2r}	0	1.0				281.0	
	0		1.0		-281.0		
	0			1.0			
	0				1.0		
	0					1.0	
	0						1.0
Φ_{2e}	15.951	-0.1684-04	-0.4919-04	-0.1213-06	0.7520-06	-0.8515-07	0.8625-04
	18.322	-0.4937-05	-0.5136-03	0.1548-04	-0.5339-04	0.4046-06	0.9722-05
	18.743	-0.5134-03	0.9652-05	0.5101-04	0.4849-06	0.5141-04	-0.7607-05
	31.821	-0.3583-02	-0.2211-05	-0.2033-04	-0.3961-07	0.5917-04	-0.4924-05
	33.268	0.3084-04	0.1385-03	0.8666-02	0.1862-05	-0.4349-06	-0.2317-06
	35.575	0.4981-04	-0.8480-02	0.1325-03	-0.7279-04	-0.3614-06	-0.1303-05
	35.742	0.2066-03	0.1477-02	-0.2137-04	0.1225-04	-0.6431-06	-0.7716-04
	36.690	-0.8300-02	0.1380-06	0.1838-04	-0.8416-08	0.4193-04	0.2706-05
	39.599	-0.1993-04	-0.2950-02	0.5960-05	0.1491-04	0.2151-06	-0.7425-05
	44.105	0.7445-03	0.3225-05	0.3253-06	-0.8849-06	-0.4060-05	-0.3422-05
	50.868	0.1148-01	-0.1448-02	-0.8008-05	-0.1013-04	-0.8209-04	-0.4467-05
	51.065	0.1546-02	0.1150-01	0.1281-04	0.7895-04	-0.1079-04	-0.2388-04
	54.416	0.6481-04	0.1769-04	0.6990-02	0.1590-05	-0.2250-05	-0.9847-07
	60.343	0.1857-02	-0.3054-05	-0.2117-04	-0.2557-06	-0.5638-04	-0.6458-05
	60.471	0.4187-04	0.1949-02	0.3156-04	0.5694-04	-0.4749-06	-0.1298-04
	70.407	0.1872-03	0.1667-04	0.4222-03	-0.3524-05	-0.5612-04	-0.2011-04
	70.492	0.3962-04	-0.6575-04	-0.1209-02	0.4899-04	-0.4406-05	-0.5142-04
	70.747	-0.5691-04	0.3175-03	0.2800-02	0.2253-04	0.1108-05	-0.2779-04
	70.829	-0.5678-04	-0.2767-03	-0.3647-03	-0.1010-04	0.3908-05	-0.4581-04
	74.051	0.6351-03	0.1827-02	0.2275-04	0.6449-05	0.4414-05	0.5020-03
	89.907	-0.1016-01	0.1230-01	-0.2931-02	-0.5806-04	-0.4582-04	-0.4424-05
	90.807	0.1271-01	0.1012-01	0.4637-03	-0.5022-04	0.6175-04	-0.5466-04
	93.490	-0.2332-02	0.1656-02	0.1734-01	0.6823-05	-0.1961-04	0.6899-06
	136.36	0.1333-02	-0.9762-02	-0.4095-03	0.4804-03	0.6433-04	-0.9210-04

Table 21. Rigid Body Mass Matrix $[M_{rr}]$ for MECO Centaur/ATS Model

	X	Y	Z	θ_x	θ_y	θ_z
X	0.15244+02	0.46438-11	-0.31024-05	0.13140-05	0.27308+04	-0.68457+01
Y	0.46422-11	0.15247+02	-0.10988-05	-0.27288+04	- 0.13185-05	0.16467+02
Z	-0.31025-05	0.10989-05	-0.15285+02	6.8457	-16.467	0.00000
θ_x	0.13141-05	-0.27288+04	6.846	0.81253+06	0.10511+03	-0.20202+04
θ_y	0.27308+04	-0.13186-05	-16.467	0.10511+03	0.81299+06	0.84467+03
θ_z	-0.68457+01	0.16467+02	0.00000	-0.20202+04	0.84467+03	0.18929+05